Proceedings of the 17th World Congress
The International Federation of Automatic Control
Seoul, Korea, July 6-11, 2008

Position Error Signal based Control Designs for Control of Self-servo Track Writer

Sehoon Oh and Yoichi Hori *

* *Institute of Industrial Science, University of Tokyo, Japan (Tel: 81-3-5452-6289; e-mail: sehoon@horilab.iis.u-tokyo.ac.jp).*

Abstract: Among the many problems in the Self-servo Track Writer (SSTW), the error propagation problem is discussed in this paper. To deal with the error propagation problem, we take two approaches: estimation of the absolute head position and reference correction design using the Position Error Signal (PES) in the previous track.
To improve the estimation of absolute position of the head with regard to the whole disc, Kalman filter is designed and removes the estimation error caused by the sensor noise in PES. For the reference correction design problem, a transition matrix which can describe the error propagation characteristics of SSTW is derived and utilized for reference correction for the next servowriting. Simulations results verify the effectiveness of two suggestions.

Keywords: Hard Disk Drive, Self Servo Track Writer, Error propagation, Kalman filter, Loop shaping

1. INTRODUCTION

1.1 Necessity of Self Servo Track Writer

Hard-disk Drives are, recently, used not only for the computer system but also for consumer electronics such as hard-disk recorder and car navigation system. This requests higher track density which leads to larger time to write the servo tracks. This increase in the number of servo tracks also cost an enormous investment to secure sufficient facilities such as clean room spaces. This situation forces manufactures to develop novel servo track writing (STW) technologies such as non-contact STW, media STW, self STW, and pattern printing STW.

Among these technologies, self servo track writer (SSTW) uses the read and write elements which is already installed in the read/write head of the hard disk drives. This makes the servo track writing process be achieved without an external servowriting machine and consequently reduces time and cost (Szita [2003], Kang et al. [2005]).

The SSTW uses the offset between the read and write elements of the head. At first, guide servo track patterns are written on a disc drive, then a new servo track is written with the write elements of the head while the read elements reads the previously-written servo track. This is self-propagating of servo track writing.

This self-propagation, however, has several drawbacks. Among them, the most important problem is error propagation. If there is some error in servo tracks, for example, a written servo track cannot be written in a perfect circular form; the error also will be propagated through the self servo track writing process.

The causes of this problem can be listed as follows (Yarmchuk [1999], Bando and Hori [2004]):

(1) High gain greater than unity in the complimentary sensitivity function especially in high frequency band
(2) Disturbances and noises in hard disk drive system
(3) Limited measurable output signal

1.2 Main purpose of this research

It is true that there are several other problems in SSTW other than this error propagation problem, only the error propagation problem, however, is focused on in this paper.

This paper is organized as follows; at first, the dynamics of the SSTW is modeled and based on that dynamics, the error propagation characteristic is analyzed in Session 2. Then in Session 3, a method to depress the error propagation is proposed using estimation of the absolute head position. Kalman filter is adopted and shows some improvements comparing with the conventional method. Lastly, Session 4 analyzes the propagation characteristics in frequency domain, and reflect in correction of reference for the next servowriting. Simulation results in Session 5 verify our analysis and design method.

2. MODELING OF SELF SERVO TRACK WRITER AND FORMULIZATION OF THE PROBLEM

As explained in the previous session, the SSTW uses the writing element and read element in the head; it writes new servo track, tracking the previous servo track signals and repeats the same process. Since the SSTW tracks previous servo tracks when it writes new track, the control for the SSTW can be the same with the conventional following control.

2.1 Modeling of SSTW

Figure 1 shows the propagation characteristics in the SSTW as a block diagram.

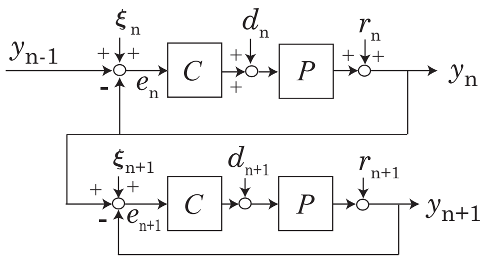

Fig. 1. Propagation in Self-servo Track Writer

One loop consisting of a plant P and a controller C represents the following controlled system loop. All the symbols used in figures and remainder of this paper are explained in Table 1.

Table 1. Definition of Symbols

y	Absolute position of the head
Δy	Position error from the ideal circle track
ξ	Sensor noise in Position Error Signal
u^{ff}	Reference correction
d	Torque disturbance
r	Repeatable runout (RRO) w/ flutter noise
N	Equivalent disturbance
e	Position Error Signal (PES)
E^a	Absolute track squeeze error
E^r	Relative track squeeze error
n(subscript)	nth track
KF(superscript)	related with Kalman Filter

Note that the offset between write element and read element in the head in Figure 1 is assumed to be zero in the remainder of this paper to simplify the analysis.

The absolute head position y_n in nth track is given to $(n+1)$th track as a position reference; this is the propagation characteristic is the SSTW.

2.2 Error Propagation in SSTW

Due to the propagation characteristics in the SSTW, errors caused by mechanical disturbances in one track are reproduced from one track to the next. Although the feedback controller (C in Figure 1) suppresses those disturbances it cannot eliminate the disturbances perfectly. The output error caused by the unsuppressed disturbances will be propagated or even amplified as the track number increases.

For example, the disturbance d_n in the input terminal is attenuated in the output y_n with the characteristic of $\frac{P}{1+PC}$ in nth track. d_n remaining in y_n will be propagated to y_{n+1} with the characteristic of $\frac{PC}{1+PC}$, which means if the remaining d_n is in the bandwidth of $\frac{PC}{1+PC}$, it will not be deleted forever. The disturbance will be even amplified in the frequency range where the amplitude of the complementary sensitivity function becomes greater than 1 due to the waterbed characteristics.

The SSTW cannot be realized without solving this error propagation problem. For this end, this paper suggests control designs which suppress these propagating errors using the measurable position error signals.

2.3 Simulation using Benchmark Problem

This paper adopts a benchmark problem software (MSS [2005]) to analyze and simulate the proposed control algorithm. This benchmark software has been developed by a working group in the Institute of Electrical Engineers of Japan -Technical Committee for Mass Storage Servo Control.

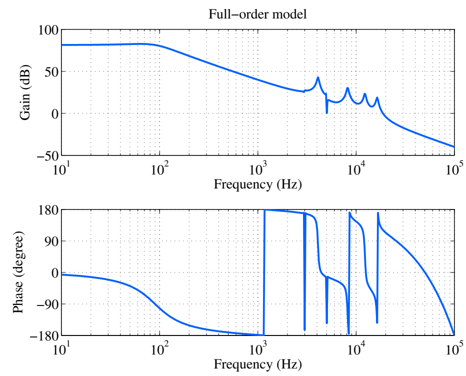

Fig. 3. Frequency Response of VCM Model

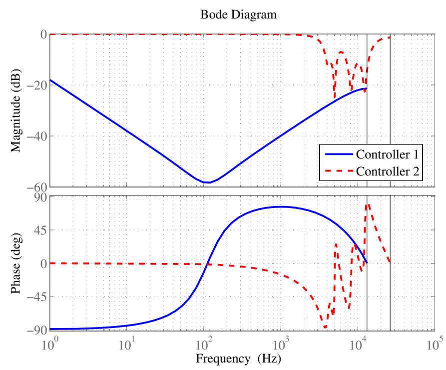

Fig. 4. Frequency Response of Controller

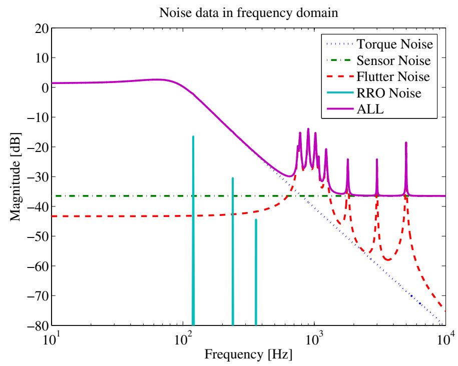

Fig. 5. Frequency Characteritics of Disturbances

Figure 2 is the block diagram which simulates motion of the head in track writing for one track. With this simulation for one track, the absolute head position Y and the position error signal PES are stored and the stored values are used as the reference and the source for the correction of the reference for the next servowriting.

Figure 3 to Figure 5 are the frequency characteristics of the VCM, two feedback controllers and the disturbances

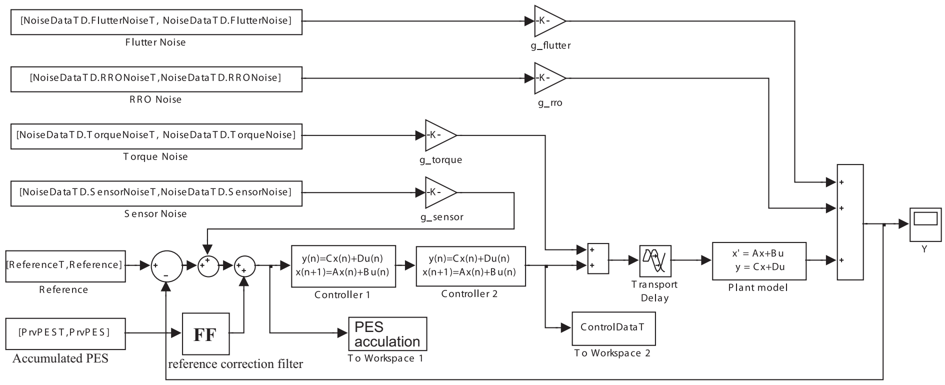

Fig. 2. Block-diagram of Benchmark Simulation

which are used in the benchmark problem software. Feedback controller consists of two multirated digital controllers: a discrete PID control and a notch filter which has twice sampling time compared with the PES sampling time($37.8\mu s$). All the disturbance are produced based on random numbers. RRO noise is given in the same time pattern through all track writings.

The FF block in Figure 2 is a reference correction filter which uses the PES accumulated to the last track as its input. Proper design of this FF can suppress the error propagation. To discuss this design is the main purpose of this paper.

Evaluation of the error propagation is done using 3σ (three times of the standard deviation) of Y and PES, as 0 in Y is assumed to be the center of each track. 3σ of Y evaluates the absolute track squeeze error and 3σ of PES evaluates the relative track squeeze error.

For the comparison with the error propagation suppression control which will be suggested in the following sessions, 3σ of Y and PES without control are illustrated in Figure 6 based on simulations.

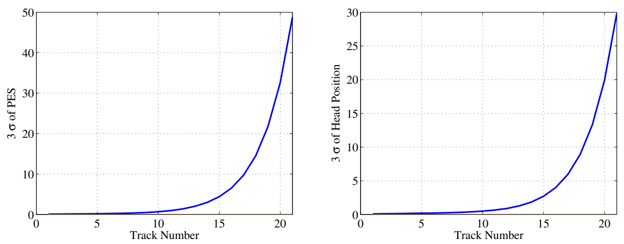

(a) PES (b) Head Position

Fig. 6. Transitions of 3σ of PES (a) and Head Position (b)

This simulation reveals that both 3σ increases exponentially with reference to the track numbers without any reference correction.

3. KALMAN FILTER DESIGN FOR ERROR PROPAGATION CONTROL

In self servo track writing process, the only measurable signal in each track is position error signal which is the error between the current head position and the previously-written servo track. This PES is relative error between two servo tracks but not an absolute error from the track that should be written - a concentric circle with the same distances from other circles; this is one cause of the error propagation characteristics.

For this reason, the absolute error is needed to be observed in order to error propagation and it is another interpretation of the reference correction which sets FF in Figure 2 as 1.

In this session, an improved absolute head estimation method is suggested.

3.1 Estimation by Linear Addition of PES

Equation (2) is an algorithm to estimate the absolute position head suggested in Bando and Hori [2004].

$$e_n[k] = y_{n-1}[k] - y_n[k] + \frac{1}{1+PC}\xi_n[k] \tag{1}$$

$$\sum_{i=1}^{n} e_i[k] = y_0[k] - y_n[k] + \sum_{i=1}^{n}\left(\frac{1}{1+PC}\right)^i \xi_i[k]$$
$$= \Delta\hat{y}_n[k] = u_{n+1}^{ff}[k] \tag{2}$$

Since each PES has information on its own error from the previous servo track, the absolute error of current head position can be estimated by accumulating PESs in the previous tracks. Then, the estimated absolute error $\Delta\hat{y}_n[k]$ is used as a reference correction to the next servo track writing, which will compensate the absolute error.

This estimation, however, also accumulates the measurement noise which increases 3σ of Y and PES (Bando and Hori [2004]) and cannot completely prevent the error propagation due to the noise (Melkote et al. [2002]).

3.2 Effect of Measurement Noise in Head Position Estimation

With the feedfoward control of Equation (2), the error to be attenuated will be $e_n[k] + u_n^{ff}[k]$ in Equation (3)

$$e_n[k] + u_n^{ff}[k] = y_0[k] - y_n[k] + \sum_{i=1}^{n}\left(\frac{1}{1+PC}\right)^i \xi_i[k]$$

(3)

As this is the estimated absolute track squeeze error, the head position of $(n+1)$th track can be positioned on the correct circle like Equation (4) in the bandwidth of feedback controller.

$$y_n[k] \rightarrow y_0[k] + \sum_{i=1}^{n} \left(\frac{1}{1+PC} \right)^i \xi_i[k] \tag{4}$$

The problem is the second term; the accumulation of the measurement noise. Even though the mean value of the measurement noise is zero, the variance increases in this accumulation. This is the propagation of measurement noise.

Simulation indicates this characteristic.

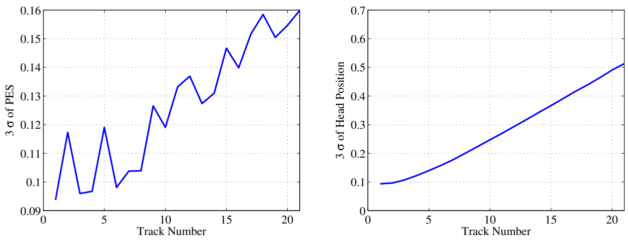

(a) PES (b) Head Position

Fig. 7. Transitions of 3σ of PES and Head Position

Figure 7 is the result. 3σ of Y and PES are increasing w.r.t the track number although the slope becomes smaller than Figure 6. This result reveals that the head position estimation by accumulating the PES can suppress to some extent but cannot eliminate it.

Bando and Hori [2004] also discusses that by multiplying a gain less than 1, the propagation can be suppressed more, which can be related to research on the proper design of FF in Figure 2.

3.3 Accurate Head Position Estimation by Kalman Filter Design

To remove the effect of the measurement noise, a Kalman filter is designed for correct estimation of the absolute head position. The dynamics from y_n to y_{n+1} is used for the dynamics of the Kalman filter design. VCM is modeled as a second order nominal model and the notch filters in the feedback controller are not included in this dynamics for simplification.

The states $\boldsymbol{x}_n^{KF}$ in Equation (5) has 5 states; 2 from the VCM and 3 from the PID controller.

$$\begin{aligned} \boldsymbol{x}_n^{KF}[k+1] &= A\boldsymbol{x}_n^{KF}[k] + \boldsymbol{B}\boldsymbol{u}_n^{KF}[k] + \boldsymbol{G}\boldsymbol{w}_n^{KF}[k] \\ y_n^{KF}[k] &= \boldsymbol{C}\boldsymbol{x}_n^{KF}[k] + \boldsymbol{B}\boldsymbol{u}_n^{KF}[k] + \boldsymbol{H}\boldsymbol{w}_n^{KF}[k] + v_n[k] \end{aligned} \tag{5}$$

The input u_n^{KF} is the signal to the PID controller. Since the reference position can be assumed to be 0 ignoring the offset between the write element and read element of the head, the reference correction $u_n^{ff}[k]$ will be this input u_n^{KF}. The measurable signal PES is used as the output $\boldsymbol{y}_n^{KF}[k]$ of the dynamics. The output noise v and the system noise $\boldsymbol{w}^{KF}$ are introduced to design the Kalman filte gain.

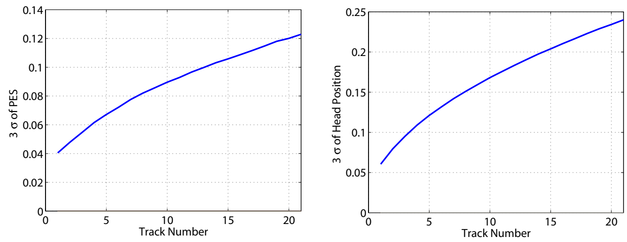

(a) PES (b) Head Position

Fig. 8. 3σ of PES and Head Position with gain 1

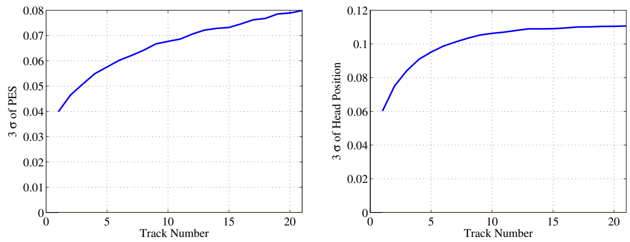

(a) PES (b) Head Position

Fig. 9. 3σ of PES and Head Position with gain 0.88

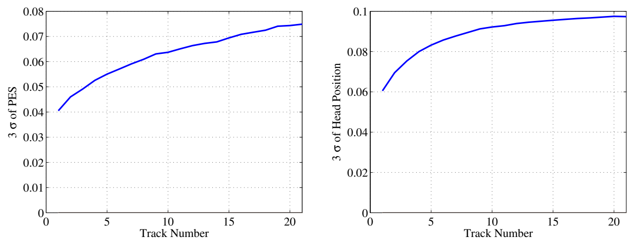

(a) PES (b) Head Position

Fig. 10. 3σ of PES and Head Position w/ gain 0.88 and Kalman Filter

The measurement noise can be took into considereation using these two kinds of noise.

Considering these relationships, the Kalman filter is designed as Equation (6). The estimated relative error $\hat{e}_n[k]$ is accumulated for the reference correction in the next track.

$$\begin{aligned} \hat{\boldsymbol{x}}_n^{KF}[k+1] &= A\hat{\boldsymbol{x}}_n^{KF}[k] + \boldsymbol{B}u_n^{ff}[k] \\ &\quad + \boldsymbol{L}\Big(PES_n[k] + u_n^{ff}[k] - \boldsymbol{C}\hat{\boldsymbol{x}}_n^{KF}[k] - \boldsymbol{D}u_n^{ff}[k]\Big) \\ \hat{e}_n[k] + \hat{u}_n^{ff}[k] &= \hat{y}_n^{KF}[k] = \boldsymbol{C}\hat{\boldsymbol{x}}_n^{KF}[k] + \boldsymbol{D}u_n^{ff}[k] \end{aligned} \tag{6}$$

$\boldsymbol{L}$ is the Kalman filter gain designed based on the covariance of $\boldsymbol{w}^{KF}$ and v in Equation (5). Note that the measurement noise ξ works not only as the output noise v but also the system noise $\boldsymbol{w}^{KF}$.

In Kalman filter design, v does not affects the states but it only affects the measurement. ξ, however, affects the states $\boldsymbol{x}^{KF}$, since it is fed back to the feedback controller. Considering this point, one of the columns in $\boldsymbol{G}$ in Equation(5) is designed as the same with $\boldsymbol{B}$.

Figure 8 to 10 are simulation results of Kalman filter. In order to explore the effectiveness of Kalman filter to ξ, simplified simulations are conducted. Flutter Noise and RRO Noise in Figure 2 are removed in these simulations and the measurement noise and torque disturbance are applied.

The reference correction filter FF changes from the gain 1 to 0.88. Figure 8 and 9 are comparison between the result of the gain 1 and 0.88. The gain 1 shows the best propagation suppression performance with all the disturbance including Flutter Noise and RRO Noise. However, when those disturbances are removed, the gain 0.88 shows the best performance.

This change in the best gain can be explained by the frequency characteristics of disturbances. The removed disturbances are in the high frequency range, which shows that higher gain is necessary to suppress the error propagation in the high frequency range. On the other hand, for the disturbances in the low frequency range such as measurement noise and torque disturbance, the lower gain near 0.88 becomes the best gain. Figure 8 to 10 verifies this point.

Figure 10 is the result with the Kalman filter and the gain 0.88. Compared with Figure 10, the error propagation is suppressed more. Design of K should be more explored to obtain better suppression performance.

4. REFERENCE CORRECTION DESIGN BASED ON THE FREQUENCY CHARACTERISTICS OF ERROR PROPAGATION

In this session, reference correction (which is desigend by the FF in Figure 2) design is discussed. This approach is different form the estimation of the head position and also can be combined with the head position estimation suggested in the previous session. Du et al. [2005] is one of these approaches. This approach can also be interpreted as iterative learning control or repetitive control (Chen et al. [2006]) as it uses the signals in the previous execution.

4.1 Derivation of Propagation Characteristic Function

Figure 11 shows the block diagram of the reference correction in SSTW. Measured data in the previous track is filtered and provided as a refenrece correction in the next track.

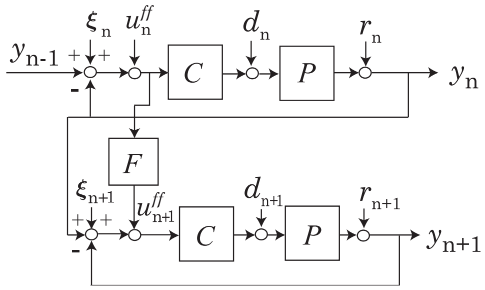

Fig. 11. SSTW Control using Reference Correction

It is another interesting point that the estimation of head position by accumulating the PES can be categorized as this reference correction which sets F to 1 or 0.88.

The transition matrix on how two variables u^{ff} and y propagate is calculated as Equation (7).

$$\begin{pmatrix} u^{ff}_{n+1}[k] \\ y_n[k] \end{pmatrix} = \begin{pmatrix} F(1-T) & F(1-T) \\ T & T \end{pmatrix} \begin{pmatrix} u^{ff}_n[k] \\ y_{n-1}[k] \end{pmatrix} \quad (7)$$

From this matrix, the relationship between u^{ff}_n and y_{n-1} is given as

$$Tu^{ff}_n[k] = F(1-T)y_{n-1}[k]. \quad (8)$$

This simplifies the propagation characteristics as the below equation.

$$y_{n+1} = (T + F - TF)y_n \quad (9)$$

Error propagation can be suppressed by shaping this propagation characteristics; $T+F-TF$. Using the descriptions C, P in Figure 11, the propagation characteristics can be described as

$$T + F(1-T) = \frac{CP}{1+CP} + \frac{F}{1+CP} = T_{pr}. \quad (10)$$

The reference correction filter F can be designed based on this equation. If F is designed to make the infinity norm of T_{pr} less than unity, error propagation will be converged to zero, which is proved in the iterative learning control theory Bristow et al. [2006].

4.2 Analysis of Propagation Characteristics of Track Errors

In this subsection, propagation characteristics of two track errors are analyzed: the absolute track squeeze error and the relative track squeeze error. The effect of disturbance and noise to these two errors are focused.

The disturbance and noise described in Figure 5 - torque disturbance, flutter noise, RRO noise and sensor noise - are considered in the propagation analysis. In the remainder of this paper, all noises except the sensor noise are dealt with as one equivalent noise which is applied to the output of the plant and described as N while the sensor noise is described as ξ.

The absolute track squeeze error, E^a can be given as $-y[k]$ since the reference position for each track is assumed to be zero. Its propagation is described as Equation(11). Equation (11) is the case of the relative track squeeze error E^r.

$$\begin{aligned} E^a_{n+1}[k] &= T_{pr}E^a_n[k] - FSN_n[k] + SN_{n+1}[k] + T\xi_{n+1}[k] \\ E^r_{n+1}[k] &= T_{pr}E^r_n[k] - FS(N_{n-1}[k] - N_n[k]) \\ &\quad + S(N_n[k] - N_{n+1}[k]) + T(\xi_n[k] - \xi_{n+1}[k]) \quad (11) \end{aligned}$$

The absolute squeeze error is excited by N and ξ through $(1-F)$ and T respectively. Note that F will affect not only the propagation characteristics T_{pr} but also the way the noise N excites the absolute track squeeze error.

Comparing Equation (11), the relative track error is excited by the difference of the noise between the previous track and the current track.

5. SIMULATION OF PROPOSED REFERENCE CORRECTION USING BENCHMARK PROBLEM

Based on Equation (10), F is designed as Equation (12) to decrease the norm of T_{pr} under unity, with the gain K between 0 and 1;

$$F = K + (K-1)CP_n, \quad (12)$$

$$T_{pr} = T + F(1-T) = K \quad (13)$$

where P_n is the nominal dynamics of VCM which consists of a second order system. This F makes the propagation characteristic T_{pr} in Equation (10) K if $P_n = P$.

Simulations are done changing K from 0.9 to 1.1; All the internal states in the overall system is reset to 0 at the start of each iteration and the values of PES and the output (Reference and Accumulated PES in Figure 2) only are transmitted to the next iteration. The seeds for the random noises (Flutter Noise, Torque Noise, Sensor Noise in Figure 2) are changed for every iteration. The results are illustrated in Figure 12.

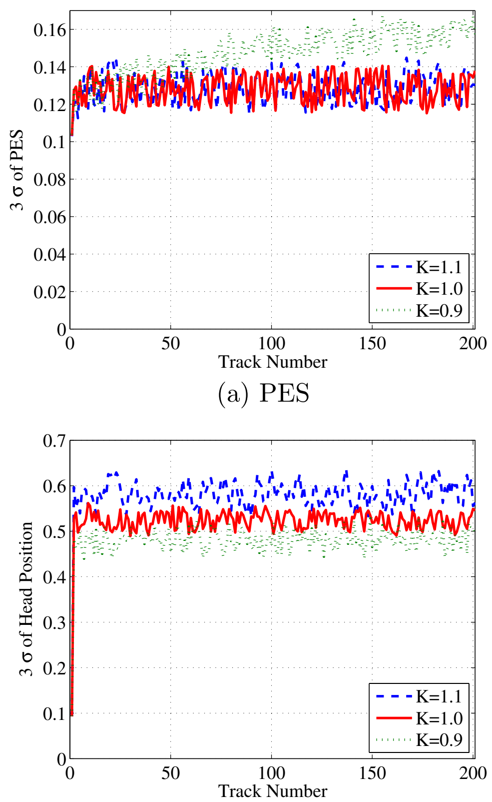

(a) PES

(b) Head Position

Fig. 12. 3σ of PES and Head Position (w/ FF control)

Simulations are conducted until the track reaches 200th track. Both the relative track error and absolute track error do not diverge and converge to particular values when K is 1.1 and 1.0. From this simulation result, the gain 1 can be chosen as the optimal gain, which will also minimize the norm of T_{pr} ideally.

Another noticeable point in this simulation is the difference between converged values of two errors. The relative track error converges around 0.13 while the absolute track error converges around 0.55. Relative track error is more important in terms of practical use. If the distance between adjacent tracks is constant with small deviation, it can be used as servo track although the absolute shape of the track is not a perfect circle.

The cause of different converged values of two errors and how to decrease those values are to be researched further.

6. CONCLUSION

This paper focuses on the propagation characteristics of SSTW and suggests several solutions to deal with the propagation problem: accurate estimation of the absolute head position based on Kalman filter design and a reference correction design based on the analysis of the propagation characteristic in the frequency domain.

The benchmark problem software developed by the Institute of Electrical Engineers of Japan is adopted for the precise simulation.

As for the estimation of the absolute head position design, the simulation results show the effectiveness of Kalman filter design on the measurement noise. To design effective reference correction filter, the propagation characteristics in the SSTW is analyzed in mathematical ways. The proposed reference correction based on that propagation characteristic succeeded to eliminate the error propagation.

As future work, how to control the value to which the error converges should be explored.

REFERENCES

G. Szita. Servo track writing using extended copying with head offset. *US Patent*, US 6,631,046 B2, 2003.

E. Yarmchuk, T. Chainer, M.D. Schultz and B. Webb, Radial self-propagation pattern generation for disk file servowriting. *US Patent*, US Patent 5,907,447, 1999.

N. Bando and Y. Hori. Estimation of the Head Position for Self Servo Track Writer and Application of PTC. (in Japanese) in *IEE of Japan Technical Meeting Record*, IIC-04-72C2004.

Technical Committee for Mass Storage Servo Control. http://mizugaki.iis.u-tokyo.ac.jp/nss/MSS_bench.htm

H. Ye, V. Sng, C. Du, J. Zhang and G. Guo. Radial Error Propagation Issues in Self-servo Track Writing Technology. *IEEE Transactions on Magnetics*, volume 38, number 5, pages 2180- 2182, 2002.

C. Du, J. Zhang and G. Guo. Disturbance Modeling and Control Design for Self-servo Track Writing. *IEEE/ASME Transactions on Mechatronics*, volume 10, number 1, pages 122-127, 2005.

C. Kang and C. Kim, An iterative learning approach to compensation for the servo track writing error in high track density disk drives *Microsystem Technology*, volume 11, pages 623–637, 2005.

Y. Chen, K.L. Moore, J. Yu, T. Zhang, Iterative learning control and repetitive control in hard disk drive industry - A tutorial *in the Proc. of IEEE Conference on Decision and Control*, pages. 2338-2351, 2006.

D.A.Bristow, M.Tharayil, A.G.Alleyne, A survey of iterative learning control *IEEE Control Systems Magazine*, volume 26, number 3, pages. 96- 114, 2006.

H. Melkote, R.J. McNab, Modeling and control for self-servowriting in hard disk drives: a repetitive process approach *in the Proc. of American Control Conference*, pages. 2005-2010, 2006

H Melkote, R McNab, B Cloke, V Agarwal A study of radial error propagation and self servowriting in disk dirives *in the Proc. of American Control Conference*, pages. 1372-1377, 2002